Image reconstruction in ultrasound-modulated optical tomography

Jun Li, Lihong V. Wang

Jun Li, Lihong V. Wang, "Image reconstruction in ultrasound-modulated optical tomography," Proc. SPIE 5320, Photons Plus Ultrasound: Imaging and Sensing, (12 July 2004); doi: 10.1117/12.530537

SPIE.

Event: Biomedical Optics 2004, 2004, San Jose, CA, United States

Image reconstruction in ultrasound-modulated optical tomography

Jun Li and Lihong V. Wang*
Optical Imaging Laboratory, Department of Biomedical Engineering
Texas A&M University, College Station, TX 77843-3120

Abstract

We present an image reconstruction technique for ultrasound-modulated optical tomography. It is the first time, to the authors' knowledge, that a reconstruction technique is developed for such tomography. In analogy to X-ray computed tomography, an ultrasonic beam is scanned linearly and angularly across a biological-tissue sample. Ultrasound-modulated optical signals, reflecting the optical properties of the sample inside the ultrasonic column, are detected and taken as the projection data for the reconstruction, where a filtered back-projection algorithm is implemented. With the technique, two-dimensional images of biological tissues in cross-sections containing the scanned ultrasonic axis are obtained. The image resolution is determined by the diameter of the ultrasonic focal zone. The technique can be implemented with any standard signal-detection scheme for ultrasonic modulation of coherent light in scattering media and can be applied directly to achieve three-dimensional images of biological tissues.
Keywords: ultrasound, optical, tomography, modulate, reconstruction

1. INTRODUCTION

Taking advantage of optical contrast and ultrasonic resolution, ultrasound-modulated optical tomography[1–3] is an attractive technique in the biomedical optical imaging field. In this technique, an ultrasonic beam is focused into biological tissue to modulate the coherent light crossing over the ultrasonic beam in the tissue. Because ultrasound is scattered much less than light in biological tissue, it can provide good spatial information for imaging in the optical diffusion regime. By detecting the ultrasound-modulated light, the optical properties related to the ultrasound location inside the tissue can be derived. Poor optical resolution, resulting from strong optical scattering of biological tissues, is avoided. By scanning a sample or an ultrasonic beam, one-dimensional (1D) or two-dimensional (2D) images of a cross-section perpendicular to the ultrasonic axis can be obtained directly. To obtain an image of a cross-section containing the ultrasonic axis, Leveque-Fort[4] reported scanning of an ultrasonic beam axially; however, the resolution was poor because the axial dimension of the ultrasonic focal zone was quite long. Wang *et al.*[5] and Yao *et al.*[6] developed a technique called frequency-swept ultrasound-modulated optical tomography and achieved controllable spatial resolution along the ultrasonic axis; this method was further studied recently by Forget *et al.*[7] But so far, to the authors' knowledge, no reconstruction algorithms have been employed in ultrasound-modulated optical tomography.

In this paper, we report a novel imaging technique: ultrasound-modulated optical computed tomography (UMOCT). The technique was developed with inspiration from X-ray computed tomography (CT). In X-ray CT, through multiple linear and angular scans across a sample carried out with an X-ray source-detector pair, a cross-sectional image of the sample is reconstructed from the detected X-ray intensities, which reflect the attenuation properties along the X-ray paths in the sample. In ultrasound-modulated optical tomography, ultrasound-modulated optical signals are generated in the volume that is occupied by the ultrasonic beam in the sample. Intensities of the ultrasound-modulated optical signals reflect the optical properties (optical absorption and scattering) in this volume. Motivated by the analogy with X-ray CT, we developed the UMOCT in which a filtered back-projection algorithm was applied to reconstruct images of cross-sections formed by the scanned ultrasonic axis. It should be noted that, in UMOCT, the scanning beam was an ultrasonic beam, and the signals to be detected were diffuse optical signals.

*lwang@tamu.edu; phone 1 979 847-9040; fax 1 979 845-4450

Photons Plus Ultrasound: Imaging and Sensing, edited by
Alexander A. Oraevsky, Lihong V. Wang, Proceedings of SPIE Vol. 5320
(SPIE, Bellingham, WA, 2004) 1605-7422/04/$15 · doi: 10.1117/12.530537

2. EXPERIMENTS

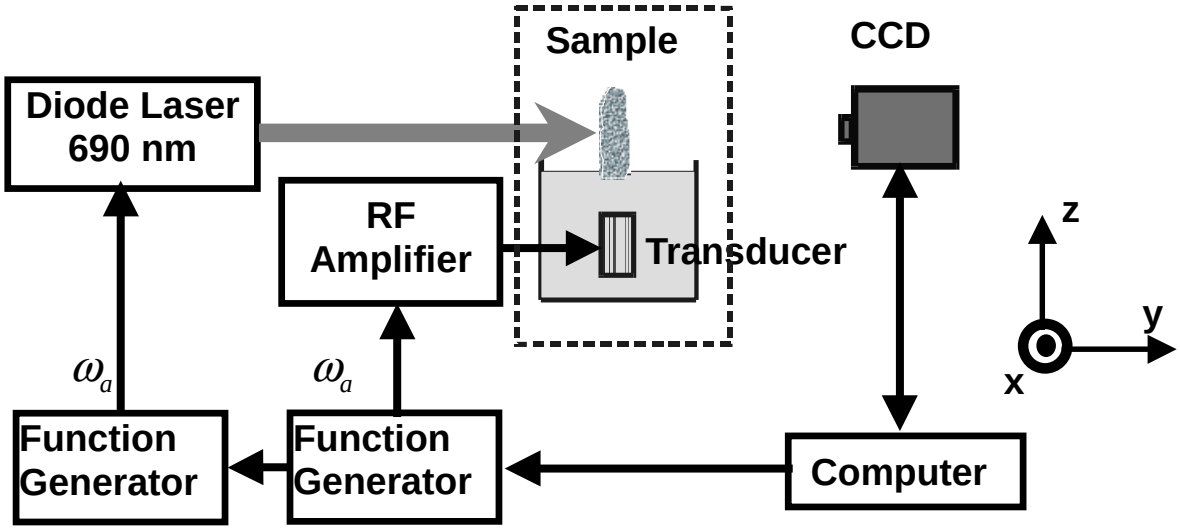

Fig. 1. Schematic of the experimental setup.

Figure 1 shows a schematic of the experimental setup. Any signal-detection schemes used in conventional ultrasound-modulated optical tomography, such as detection with a single detector or multiple detectors (i.e., parallel speckle detection[1,3] or speckle contrast detection[8]), can be employed in UMOCT. In this study, we adopted the parallel speckle detection scheme. The hardware and the extraction of ultrasound-modulated signals were similar to those in Ref. 3. In Fig. 1, a laboratory coordinate system is shown. The optical axis was along the *y* axis, and the ultrasonic axis was along the *z* axis. A laser beam of 690 nm in wavelength and 11 mW in power from a diode laser (Melles Griot, 56IMS667) was expanded to 20 mm in diameter to illuminate the sample perpendicularly. The intensity of the laser beam was modulated at the same frequency as the ultrasound. The coherence length of the laser was ~6 cm when it was modulated at 1 MHz. Ultrasonic waves, generated by a focused ultrasonic transducer (UltranLab, VHP100-1-R38) with a 38-mm focal length in water and a 1-MHz central response frequency, were coupled into the tissue sample through water in which the sample was partially immersed. The focal zone of the ultrasonic waves was 2 mm in diameter and 20 mm in length, in which the peak pressure was ~10^5 Pa. Speckle patterns generated by the scattered light from the tissue were detected by a 12-bit digital CCD camera (Dalsa, CA-D1-0256T) with 256×256 pixels. Ultrasound-modulated optical signals were extracted from the speckle patterns. Two function generators (Stanford Research Systems DS345) were used, which shared the same time base to ensure synchronization. The CCD camera and the function generator that drove the transducer were controlled with a computer.

An experiment with a transmission-detection configuration, in which the CCD camera and the incident laser beam were on opposite sides of the sample, as well as an experiment with a reflection-detection configuration, in which the CCD camera and the incident laser beam were on the same side of the sample, were carried out. The UMOCT required relative linear and angular scans between the sample and the ultrasound. In the experiment, the position of the ultrasonic transducer was fixed. A sample holder was made to allow the sample to be rotated around the *y* axis by a rotational stage and to be linearly scanned along the *x* axis by a stepper motor. Figure 2 shows a cross-section of the sample on the *xz* plane, which has been rotated around the *y* axis by an angle ϕ from its original orientation. A new coordinate system ($x'y'z'$) is set with the z' axis parallel to the ultrasonic beam. In the figure, the ultrasonic beam is located at a distance x' from the origin.

The detected ultrasound-modulated optical signal can be expressed as an integration of the signal coming from each segment along the z' axis $(z'-\delta z'/2, z'+\delta z'/2)$ in the ultrasonic column:

$$s(\phi, x') = \int s_{\phi,x'}(z')dz', \tag{1}$$

which is a Radon transform. The integrand can be expressed as $s_{\phi,x'}(z') = C_1 Q_{\phi,x'}(z') m_{\phi,x'}(z') G_{\phi,x'}(z')$, where C_1 is a constant; $Q_{\phi,x'}(z')$ represents the photon density in the segment centered at z', determined by the photon transport from the laser source to this segment; $m_{\phi,x'}(z')$ is the depth of ultrasonic modulation related to the optical properties at z' in the ultrasonic column; and $G_{\phi,x'}(z')$ represents the Green's function describing the transport of the ultrasound-modulated photons from this segment to the detector. In the diffusion regime, $Q_{\phi,x'}(z')$ and $G_{\phi,x'}(z')$ have a weak dependence on z'.

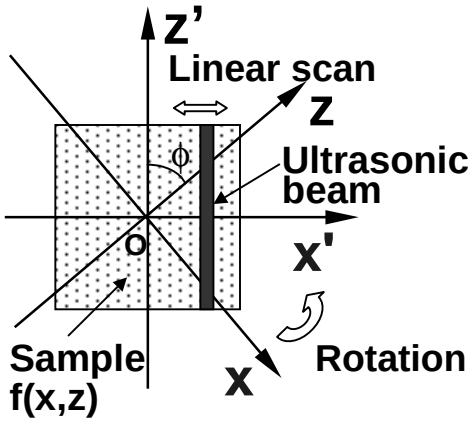

Fig 2. Cross-section of the scanning sample and the coordinate system.

The signals detected at multiple projection angles are used as the projection data for the reconstruction of an image reflecting the optical properties of the sample. The Fourier transform of the signal $s(\phi, x')$ is defined as

$$S(\phi, \omega) = \int_{-\infty}^{\infty} s(\phi, x') \exp(-i\omega x')dx', \tag{2}$$

where ω is the spatial frequency in the x' direction. The filtered back-projection was implemented with the following process: (a) filtering $S(\phi, \omega)$ with a Ram-Lak filter $|\omega|$, (b) inverse Fourier transforming the filtered signal, and (c) summing the result. The reconstructed image of the sample is expressed as

$$\hat{f}(x, z) = \int_0^{\pi} \int_{-\infty}^{\infty} S(\phi, \omega)|\omega| \exp(i\omega x')d\omega d\phi\,. \tag{3}$$

3. RESULTS

In the experiment, the step size of the linear scan along the x' axis was 1.2 mm. Biological tissue samples were used, which were made from chicken breast tissue. The object buried in background tissue samples was soft rubber or biological tissue, which had similar acoustic impedance as the background tissue and worked as optically absorbent objects. We first examined the technique in the transmission-detection configuration. Figure 2(a) shows a photograph of a cross-section of a chicken-breast-tissue sample on the xz plane. A piece of soft rubber, which had a size of ~2×2.7 mm^2 on the xz plane, was buried at 4 mm below the sample surface. Figure 2(b) shows the reconstructed image, in which the buried object is clearly seen. The size and the orientation of the object in the image are in good agreement with the actual ones.

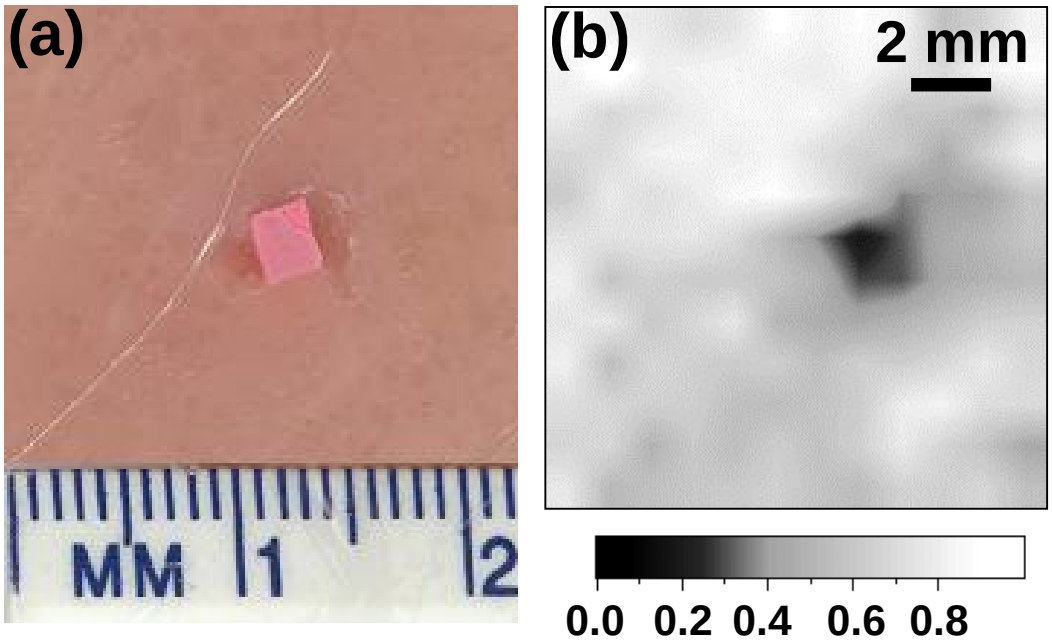

Fig. 2. Experimental result in the transmission-detection configuration. (a) Photograph of a cross-section on the *xz* plane located at 4 mm below the surface of a chicken-breast-tissue sample, in which an object made from soft rubber was buried. (b) Reconstructed 2D image.

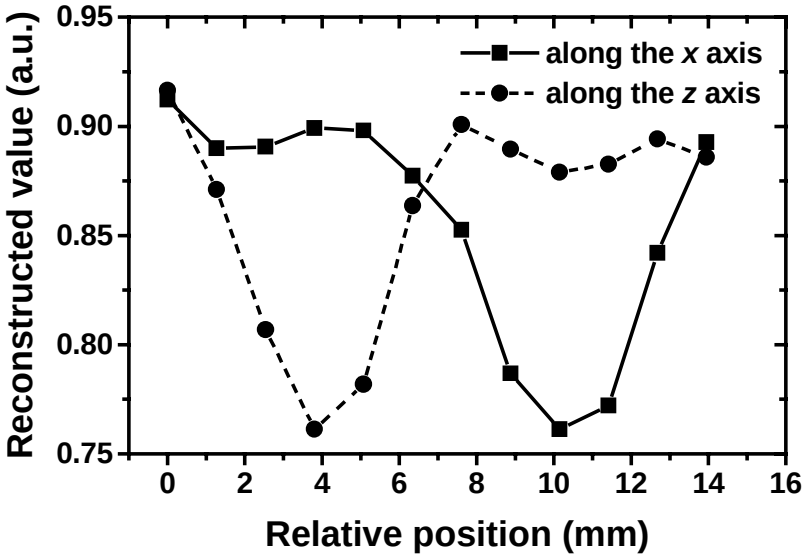

Fig. 3 Experimental result in the reflection-detection configuration. 1D images across the center of an object made from turkey muscle along the *x* axis and *z* axis, respectively. The object was buried ~9 mm deep below the surface of a chicken-breast-tissue sample.

The technique was also examined in the reflection-detection configuration. A chicken-breast-tissue sample was used, in which an object made from turkey muscle was buried ~9 mm deep in the *y* direction. The size of the object on the *xz* plane was ~4×3 mm^2. Figure 3 shows 1D images across the center of the object along the *x* and *z* axes,

respectively. We evaluated the resolution roughly with the width of the 10%-90% signal-intensity transition at the edge of the object. The widths in both of the directions were ~2 mm, which shows that the resolution in UMOCT is determined by the diameter of the ultrasonic focal zone (2 mm).

Since the reflection-detection configuration is a convenient configuration in medical imaging, the experiment implies that this technique is applicable to practical applications. In practice, it will be the ultrasonic transducer instead of the sample that will be rotated and linearly scanned. The speed of data acquisition can be improved by the use of an ultrasonic transducer array and parallel implementations.

This technique is shown to be another effective tool, in addition to frequency-swept ultrasound-modulated optical tomography, for obtaining spatial resolution along the ultrasonic axis. In frequency-swept ultrasound-modulated optical tomography, the axial resolution is determined by the frequency span of the chirp function. It has been recognized that there is a tradeoff between the resolution and the signal intensity.[6] And in that technique, an ultrasonic transducer with a broad bandwidth is required, which may not be efficient for ultrasonic modulation because of the tradeoff between transducer efficiency and bandwidth. In comparison, the resolution in UMOCT is determined by the diameter of the ultrasonic focal zone. A fine resolution can be achieved with sufficient signal intensities using a narrow-band high-efficiency ultrasonic transducer.

The method of X-ray CT has been applied in the optical regime for several years.[9,10] To the authors' knowledge, these applications have however been limited to ballistic-photon detection, i.e., ballistic imaging. Our experiments show that UMOCT extends the application of the method of X-ray CT to diffuse-light imaging with the aid of ultrasonic modulation.

4. CONCLUSTIONS

In summary, we developed a technique called ultrasound-modulated optical computed tomography and proved its feasibility experimentally in biological tissues in both optical transmission- and reflection-detection configurations. Clear images of biological tissues in cross-sections containing the scanned ultrasonic axis were obtained with a resolution of 2 mm, which was determined by the diameter of the ultrasonic focal zone. The technique can be implemented with any standard signal-detection scheme for ultrasonic modulation of coherent light in scattering media and can be applied directly to achieve three-dimensional images of biological tissues.

This project was sponsored in part by National Science Foundation grant BES-9734491; Texas Higher Education Coordinating Board grant 000512-0063-2001; and National Institutes of Health grants CA094267.

REFERENCES

1. G. Yao and L.-H. Wang, "Theoretical and experimental studies of ultrasound-modulated optical tomography in biological tissue," *Appl. Opt.* **39**, 659-664, 2000.
2. L.-H. V. Wang, "Mechanisms of ultrasonic modulation of multiply scattered coherent light: an analytic model," *Phys. Rev. Lett.* **87**, (043093) 1-4, 2001.
3. J. Li and L.-H. V. Wang, "Methods for parallel-detection-based ultrasound-modulated optical tomography," *Appl. Opt.* **41**, 2079-2084, 2002.
4. S. Leveque-Fort, "Three-dimensional acousto-optic imaging in biological tissues with parallel signal processing," *Appl. Opt.* **40**, 1029-1036, 2000.
5. L.-H. Wang, and G. Ku, "Frequency-swept ultrasound-modulated optical tomography of scattering media," *Opt. Lett.* **23**, 975-977, 1998.
6. G. Yao, S. Jiao, and L.-H. Wang, "Frequency-swept ultrasound-modulated optical tomography in biological tissue by use of parallel detection," *Opt. Lett.* **25**, 734-736, 2000.
7. B. C. Forget, F. Ramaz, M. Atlan, J. Selb, and A. C. Boccara, "High-contrast fast Fourier transform acouto-optical tomography of phantom tissues with a frequency-chirp modulation of the ultrasound," *Appl. Opt.* **42**, 1379-1383, 2003.
8. J. Li, Geng Ku and L.-H. V. Wang, "Ultrasound-modulated optical tomography of biological tissue using contrast of laser speckles," *Appl. Opt.* **41**, 6030-6035, 2002.
9. Y. Watanabe, T. Yuasa, T. Akatsuka, B. Devaraj, and H. Inaba, "Enhacement of laser CT image contrast by correction of artifacts due to surface effects," *Opt. Express* **3**, 104-110, 1998.
10. R. G. Kelly, K. J. Jordan, and J. J. Battista, "Optical CT reconstruction of 3D dose distributions using the ferrous-benzoic-xylenol (FBX) gel dosimeter," *Med. Phys.* **25**, 1741-1750, 1998.